RSC Advances

Highly transparent, bright green, sol-gel-derived monolithic silica-(Tb,Ce)PO_4 glass-ceramic phosphors

Journal:	*RSC Advances*
Manuscript ID:	RA-ART-04-2014-003559.R1
Article Type:	Paper
Date Submitted by the Author:	27-May-2014
Complete List of Authors:	Kajihara, Koich; Tokyo Metropolitan University, Department of Applied Chemistry, Graduate Scool of Urban Environmental Sciences Yamaguchi, Shiori; Tokyo Metropolitan University, Kaneko, Ken; Tokyo Metropolitan University, Kanamura, Kiyoshi; Tokyo metropolitan university,

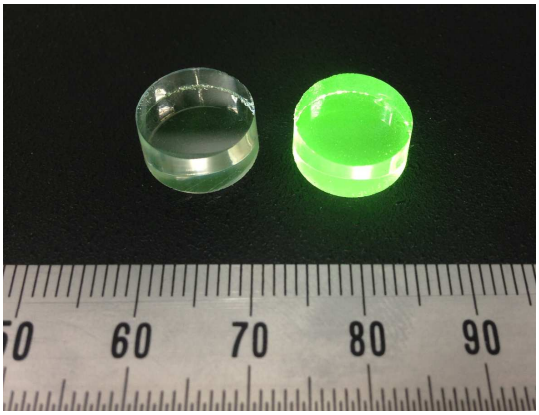

A cosolvent-free sol-gel method yields monolithic silica glasses containing (Tb,Ce)PO_4 nanocrystals, free from Rayleigh scattering, and exhibiting ultravilet-induced bright green photoluminescence.

Journal Name

RSCPublishing

ARTICLE

Highly transparent, bright green, sol-gel-derived monolithic silica-(Tb,Ce)PO_4 glass-ceramic phosphors

Cite this: DOI: 10.1039/x0xx00000x

Koichi Kajihara,[a]* Shiori Yamaguchi,[a] Ken Kaneko,[a] and Kiyoshi Kanamura[a]

Received ooth January 2012,
Accepted ooth January 2012

DOI: 10.1039/x0xx00000x

www.rsc.org/

Monolithic silica glasses containing $TbPO_4$ nanocrystals with narrow size distribution and exhibiting excellent ultraviolet (UV) transparency have been prepared using a cosolvent-free sol-gel method. Despite the high refractive index of $TbPO_4$ crystals (~1.8), observed Rayleigh scattering from the crystals is negligible because of the small average crystal size (~5 nm). The precipitated crystals are of the metastable monoclinic form, different from the stable tetragonal form. The glasses are UV photoluminescent, even at stoichiometric Tb composition, and doping with a small amount of Ce^{3+} ions increased the external quantum efficiency to ~0.76 under excitation at 290 nm. Unlike conventional glassy phosphors, the photoluminescence efficiency is high despite the high OH concentration of the glass matrix because of confinement of RE ions to the crystal phase.

Introduction

Crystals of rare-earth (RE) compounds are important for various optical components, including phosphors, scintillators, active gain media of solid-state lasers, and magneto-optical materials. Compared to monolithic single crystals, monolithic transparent glass-ceramics containing photoactive crystals have advantages that their synthesis can be easier, their shape workability is better, and metastable crystalline phases may be stabilized.[1] Silica glass is an attractive host for photoactive crystals because of the wide transparency window, which ranges from the infrared to vacuum-ultraviolet (UV) (<200 nm) spectral regions, good mechanical and chemical properties, and high radiation hardness. Crystals of RE oxides (e.g. CeO_2 [2–4] and Er_2O_3 [5]) and RE silicates (e.g. Lu_2SiO_5 [6,7]) can be precipitated by heat treatment of silica gels or glasses containing RE ions. Silica glasses containing crystals of RE fluorides, including LaF_3, YF_3, and $NaYF_4$,[8–12] have also been prepared by making use of the strong affinity of RE ions for fluorine in silica glass. However, the formation of crystals of other RE compounds has hardly been reported in silica glasses, likely because of the synthetic difficulties. In addition, unfavourable crystal growth and reactions with the silica matrix often increase scattering loss and decrease transparency of resultant glasses, particularly in the UV spectral region. We recently developed methods for synthesizing monolithic RE-doped silica glasses from solutions consisting mainly of tetraethoxysilane (TEOS) and water, without using cosolvents such as alcohols and organic solvents.[13–15] We found that codoping with phosphorus (P) effectively increases the UV transparency of RE-doped silica glasses [12] and attributed this phenomenon to the enhancement of RE ion dissolution by selective coordination of P to RE ions.[16,17] However, the mechanism of the dissolution of RE ions through P codoping has not been clarified. On the other hand, formation of RE phosphate crystals has been confirmed at high RE concentrations in RE–P–Ge codoped silica glasses prepared by a vapor-phase method.[18] Orthophosphates of RE ions are important phosphors and their nanocrystals have recently attracted attention,[19,20] whereas glass-ceramics of RE orthophosphates have only recently been reported.[21,22]

In this paper, we demonstrate the formation of nanocrystals of RE orthophosphates with narrow size distributions in RE–P codoped silica glasses by a cosolvent-free sol-gel method. Because of the small crystal size, Rayleigh scattering loss is negligible, despite the large mismatch of the refractive indices of the silica matrix and the crystals. An efficient transparent green UV phosphor has been realized by embedding (Tb,Ce)PO_4 nanocrystals, although the glass matrix contains SiOH groups at high concentrations.

Experimental procedure

A dilute aqueous solution of nitric acid was added to 25 mmol (5.2 g) of TEOS (Shin-Etsu Chemical) and stirred for 55 min at 20°C in a sealed plastic container to form a clear solution with a TEOS : H_2O : HNO_3 molar ratio of 1 : x_1 : 0.002. Triphenylphosphine oxide (TPPO) was added to this solution (TEOS : TPPO = 1 : z_P) and dissolved by stirring for another 5 min. The resultant solution was further mixed with an aqueous solution of ammonium acetate ($AcONH_4$) and RE acetates to form a solution with an overall TEOS : H_2O : HNO_3 : $AcONH_4$: TPPO:RE molar ratio of 1 : x_1+x_2 : 0.002 : y : z_P : z_{RE}, where x_1+x_2 = 10 and z_P = z_{RE}. In Ce-doped samples z_{Ce} was fixed at 0.0002 to maintain the intensity of the 4f–5d optical absorption band within the measurable range. After stirring for 1 min, the stir bar was removed and the solution was maintained at 20°C until gelation. The resultant wet gel was aged for 1 day at 60°C. The container was then opened, the solvent phase was disposed, and the gel was gently dried at

60°C. The dried gel was finally sintered in a tube furnace heated to 1200–1300°C at a rate of 200°C h^{-1} and held there for 0.5–1 h. The sintering atmosphere was changed from air to helium at 600°C. Optical absorption spectra were taken using a conventional spectrometer (U-4100, Hitachi). PL spectra were recorded using an integrating sphere (4P-GPS-053-SL, Labsphere) connected to a UV light emitting diode (LED) (~30 μW at ~290 nm) and a CCD spectrometer (EPP2000C, StellarNet) and PL intensity was calibrated using a standard lamp (LS-1-CAL, Ocean Optics). PL time decay was recorded using a silicon photodiode (S1223, Hamamatsu) connected to an oscilloscope under excitation with periodically interrupted light from another UV LED (~100 mW at ~365 nm). Several samples were crushed and subjected to X-ray diffraction (XRD) measurements (Ultima II, Rigaku) and transmission electron microscopy (TEM) studies (JEM-3200FS, JEOL, operated at 300 kV).

Results

Fig. 1(a) shows powder XRD patterns of crushed samples. The diffraction peaks of the sample prepared at z_{Tb} = 0.01 and sintered at 1200°C were obscure and the identification of the crystalline phases was not possible. The diffraction peaks became prominent with increasing the dopant concentration, sintering temperature, and sintering time. The observed pattern agreed well with that of monoclinic RE orthophosphate (monazite), which is metastable and an unusual structure for $TbPO_4$, and was dissimilar to that of the stable conventional tetragonal polymorph (xenotime).[23] Raman spectra of similarly prepared monolithic glass samples are shown in Fig. 1(b). A Raman band at ~980 cm^{-1}, attributed to the symmetric stretching mode (ν_1) of PO_4 tetrahedra in $TbPO_4$,[24] was clearly seen in both samples, and additional small bands were observed in the sample prepared at z_{Tb} = 0.02. The positions of the Raman bands of monoclinic $TbPO_4$ at ambient pressure have not been reported, and the observed bands were compared with data for monoclinic $GdPO_4$ and tetragonal $TbPO_4$.[24] The observed peak positions were similar to those of the monoclinic form rather than those of the tetragonal form, which also suggests the formation of monoclinic $TbPO_4$ nanocrystals.

Fig. 2 shows high-resolution TEM images of Ce-free and Ce-doped samples. The particles were assigned as $TbPO_4$ crystals, and the uniform diffraction contrast across each particle and clear lattice fringes indicate their good crystallinity. Histograms of particle diameters are shown in the bottom panel of Fig. 2. The average diameters and relative standard deviations (RSD), respectively, were calculated to be ~5.7 nm and ~20 % for the Ce-free sample, and ~5.1 nm and ~17 % for the Ce-doped sample. This indicates a relatively narrow particle diameter distribution. Doping with Ce at 2 at.% decreased both the average particle diameter and the size distribution; however, the reason for this is currently unknown.

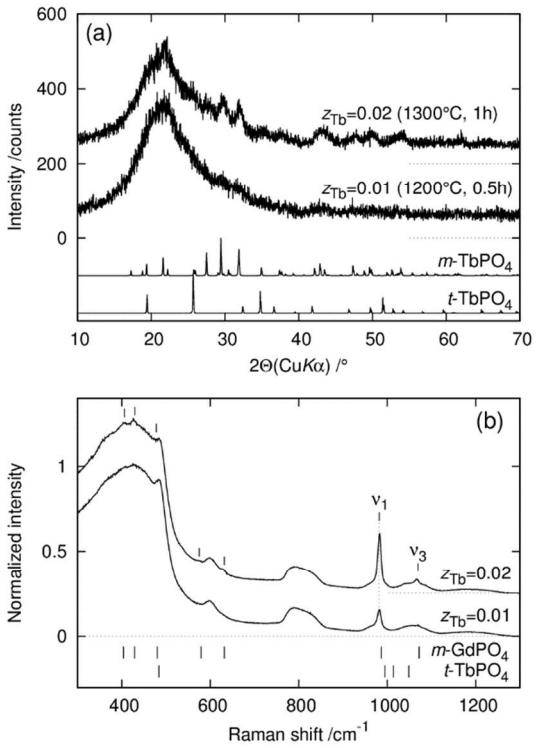

Fig. 1 (a) Powder XRD patterns and (b) Raman spectra of Ce-free samples prepared at z_{Tb} = 0.01 and sintered for 0.5 h at 1200°C, and at z_{Tb} = 0.02 and sintered for 1 h at 1300°C. Simulated XRD patterns of monoclinic and tetragonal $TbPO_4$ (*m*-$TbPO_4$ and *t*-$TbPO_4$, respectively), and peak positions of Raman bands for monoclinic $GdPO_4$ (*m*-$GdPO_4$) and *t*-$TbPO_4$ are also shown.

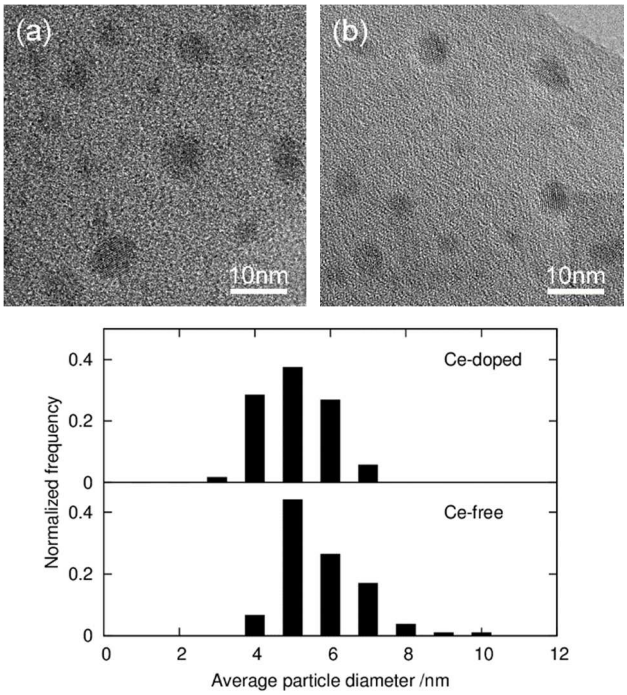

Fig. 2 (top) TEM images of Ce-free (a, z_{Ce} = 0) and Ce-doped (b, z_{Ce}/z_{RE} = 0.02) samples prepared at $z_{RE} = z_{Tb} + z_{Ce}$ = 0.01

and sintered for 0.5 h at 1200°C, and (bottom) the histograms of particle diameter distributions.

Fig. 3 shows optical absorption spectra. The Ce-free sample exhibited excellent visible and UV transparency. Because of the small crystal size shown in Fig. 2, the UV transparency was much better than glass-ceramics containing RE orthophosphates reported previously.[21,22] The absorption edge was located at ~250 nm and is attributed to the 4f–5d transition of Tb^{3+} ions.[25,26] Weak absorption bands, due to 4f–4f transitions of Tb^{3+} ions, were seen at 250–400 nm. In the Ce-doped sample, the 4f–5d transition of Ce^{3+} ions appeared in the range of 250–350 nm. The concentration of SiOH groups was evaluated from the peak intensity of the first overtone band of the SiO–H stretching mode at ~7270 cm^{-1},[13] and it was ~3.3×10^{20} cm^{-1} for the Ce-free sample and ~3.7×10^{20} cm^{-1} for the Ce-doped sample.

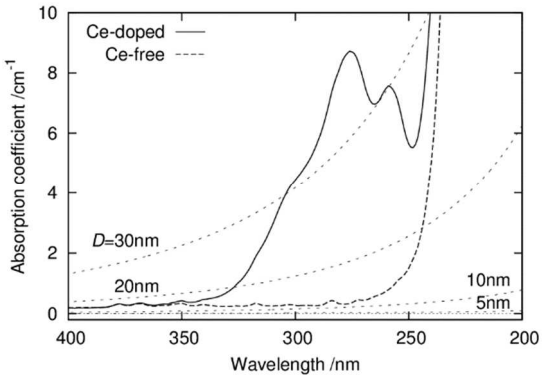

Fig. 3 Optical absorption spectra of Ce-free (z_{Ce} = 0) and Ce-doped (z_{Ce}/z_{RE} = 0.02) samples prepared at $z_{RE} = z_{Tb} + z_{Ce}$ = 0.01 and sintered for 0.5 h at 1200°C. The dotted lines show simulated optical losses due to Rayleigh scattering by spherical particles with different diameters, D, as calculated using Eq. 1.

The dotted lines in Fig. 3 indicate optical loss due to Rayleigh scattering by particles with diameters, D, of 5, 10, 20, and 30 nm. The optical loss, α, was calculated by

$$\alpha = 4\pi^4 f_v \left(\frac{m^2-1}{m^2+2}\right)^2 \frac{D^3}{\lambda^4} \quad (1)$$

The volume fraction of $TbPO_4$ crystals, f_v, was calculated to be ~0.015 when z_{Tb} = 0.01 by assuming that all Tb^{3+} ions resided within $TbPO_4$ domains. The ratio of the refractive indices of the host and the crystals, m, was approximated to be 1.23 using the refractive indices of silica glass (1.457 [27]) and $LaPO_4$ (n_x = 1.774, n_y = 1.770, and n_z = 1.828 [28]) at 633 nm since refractive indices are not available for other monazite-type RE orthophospates. Fig. 3 clearly shows that optical loss due to Rayleigh scattering is negligible when D = 5 mm, despite the large refractive index mismatch.

Fig. 4 shows photograph and PL spectra of samples used to produce Fig. 3, excited at ~290 nm. The observed PL bands were assigned to emissions from the $^5D_4$ level of Tb^{3+} ions. The emission from the $^5D_3$ level of Tb^{3+} ions was absent. The PL intensity of the Ce-doped sample was much larger than that of the Ce-free sample. Absorbance and internal and external PL quantum efficiencies can be defined by Abs = $(N_{ex}^0 - N_{ex})/N_{ex}^0$, IQE = $N_{em}/(N_{ex}^0 - N_{ex})$, and EQE = Abs×IQE = N_{em}/N_{ex}^0, respectively, where N_{ex}^0, N_{ex}, and N_{em} denote the numbers of excitation photons in an empty sphere, excitation photons not absorbed by the sample, and photons emitted from the sample, respectively. These values calculated from the spectra were Abs ≅ 0.23, IQE ≅ 0.34 and EQE ≅ 0.08 for the Ce-free sample; Abs ≅ 0.96, IQE ≅ 0.79 and EQE ≅ 0.76 for the Ce-doped sample; and Abs ≅ 0.88, IQE ≅ 0.99 and EQE ≅ 0.88 for a commercial (La,Tb,Ce)PO_4 orthophosphate phosphor powder. Thus, the Ce-doped sample exhibited remarkably strong absorption and a large EQE value.

The effect of SiOH concentrations on PL decay is shown in the inset of Fig. 4. A Ce-free sample with a low SiOH concentration was prepared by sintering at higher temperature (0.5 h at 1300°C), and its SiOH concentration was ~7×10^{19} cm^{-3}. Each PL decay curve was fitted well with a single exponential function, and the decay constant of the sample with the low SiOH concentration (~4.2 ms) was slightly larger than that of the Ce-free and Ce-doped samples with the normal SiOH concentrations (~4.0 ms for both samples), shown in the main panel. These values were larger than those recorded for (La,Tb)PO_4 (~3.3 ms) powders.[29,30] The Abs, IQE, and EQE values of the sample with the low SiOH concentration were ~0.27, ~0.30, and ~0.08, respectively, comparable to those of the sample with the Ce-free sample the with normal SiOH concentration, although the concentrations differed by a factor of ~5.

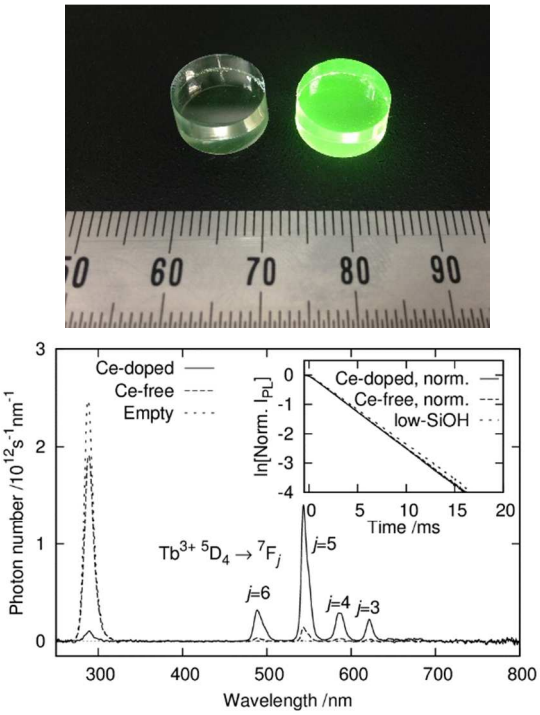

Fig. 4. (top) Photograph of Ce-free (left) and Ce-doped (right) samples used to produce Fig. 3, taken under UV exposure at ~290 nm in a light room. (bottom) PL spectra of the Ce-free and Ce-doped samples shown in the top panel. The inset shows PL decay curves for these Ce-free and Ce-doped samples, whose SiOH concentrations are normal (~3.3×10^{20} and ~3.7×10^{20} cm^{-3}, respectively), and a Ce-free sample with a low SiOH concentration (~7×10^{19} cm^{-3}) prepared at z_{Tb} = 0.01 and sintered for 0.5 h at 1300°C.

Discussion

The Tb–P codoped glasses obtained in this study show bright green PL under UV illumination. Furthermore, our previous study confirmed that this PL does not cause concentration quenching at least up to $z_{Tb} = 0.02$.[13] These observations can be explained by the presence of $TbPO_4$ crystals, whose derivatives, $(La,Tb,Ce)PO_4$, are widely used as commercial green phosphors in fluorescent lamps. However, it should be noted that PL efficiency is often very low for Tb-rich compositions, because of fast energy migration among Tb^{3+} ions and the resultant enhancement of nonradiative decay.[31] The high PL efficiency of the $TbPO_4$ nanocrystals prepared in this study is likely due to the relatively small number of Tb^{3+} ions involved in the energy transfer process (~10^3 Tb^{3+} ions in a crystal with a diameter of 5 nm), high crystallinity, and the low concentrations of killer centers both within the nanocrystals and at their surfaces. The high IQE value of green emission from Tb^{3+} ions in the Ce-doped sample (~0.79) comared with that of $(Ce,Tb)PO_4$ nanoparticles (~0.43 [19]) and $(Ce,Tb)PO_4/LaPO_4$ core-shell nanoparticles (~0.70 [20]) of comparable sizes suggests that incorporation in silica glass matrix is suitable in supressing the surface killer centers.

The observed single exponential decay kinetics of PL of Tb^{3+} ions indicates the absence of site-to-site distributions in the local environment of Tb^{3+} ions. This observation is consistent with the fact that all Tb^{3+} ions belong to the crystal phase and occupy equivalent positions in monoclinic $TbPO_4$. Although monoclinic $TbPO_4$ is metastable, it can be formed at relatively low temperatures under specific conditions and maintains its structure up to ~1000°C.[32] Thus, both the wet-chemical route employed in this study and the confinement of nanocrystals by the silica matrix plays key roles in stabilizing the monoclinic form. The monoclinic form may also be suitable for optical applications because the symmetry around the RE ions is lower than that of the tetragonal form,[23] and such reduction in symmetry generally increases the probability of transitions between 4f levels.

As shown in Fig. 3 and 4(a), Ce^{3+} ions effectively absorb UV light via the allowed 4f–5d transition and its doping significantly improves both IQE and EQE. Furthermore, the Ce^{3+} PL band typically observed at ~350 nm is missing, indicating an efficient energy transfer from Ce^{3+} to Tb^{3+} ions. This is attributed to the closeness between Ce^{3+} and Tb^{3+} ions in the $(Tb,Ce)PO_4$ crystals and a large Tb/Ce ratio (~50) in the Ce-doped sample. The absence of the emission from the $^5D_3$ level of Tb^{3+} ions is also attributed an enhancement of energy transfer (cross relatxation[33]) between Tb^{3+} ions as a result of the high Tb/RE ratio in the nanocrystals (≥0.98). Both of the disappearance of Ce^{3+} PL band and the cross relaxation between Tb^{3+} ions probably result in an enhancement of the green emission from the $^5D_4$ level of Tb^{3+} ions. Such spatial confinement of RE ions, which cannot be realized simply by dissolving RE ions in glasses, is an attractive approach to develop devices utilizing energy transfer between RE ions.

The measurement of PL quantum efficiency and Fig. 4(b) show that PL efficiency is insensitive to the concentration of SiOH groups, which commonly enhances nonradiative decay. The nonradiative decay mechanism is suppressed by the confinement of Tb^{3+} ions to $TbPO_4$ crystals, which isolates Tb^{3+} ions from SiOH groups in the silica matrix. Thus, samples with high PL efficiencies can be obtained without dehydration. This approach is suitable for developing sol-gel-derived silica-based PL devices, which generally contain SiOH groups at high concentrations.

Conclusions

We developed a wet-chemical method for the synthesis of monolithic silica glasses containing rare-earth orthophosphate nanocrystals with relatively narrow size distributions. Average crystal sizes as small as ~5 nm were achieved, making it possible to eliminate optical losses due to the Rayleigh scattering. In addition, confinement of RE ions to the nanocrystals enhances energy transfer between RE ions and suppresses nonradiative decay with SiOH groups in the glass matrix. The glasses containing $(Tb,Ce)PO_4$ nanocrystals have been shown to be bright transparent green phosphors, whose external quantum efficiencies are as high as ~86% of that of a commercial $(La,Tb,Ce)PO_4$ phosphor, despite their unoptimized RE composition and the high SiOH concentration in the glass matrix. This external quantum efficiency is one of the highest values reported for transparent inorganic phosphors. The excellent transparency is attractive for applications including scintillators and solid-state lasers, and high chemical stability and good radiation hardness of silica glass matrix is suitable for developing phosphors used under intense radiation and severe environmental conditions. This method provides a unique opportunity to produce optofunctionalized silica glasses by sol-gel methods.

Acknowledgements

We wish to thank Mr. Eiichi Watanabe of Tokyo Metropolitan University for assistance with TEM observations, and Nichia Corporation for providing their commercial $(La,Tb,Ce)PO_4$ orthophosphate phosphor powder for fluorescent lamps. This work was partly supported by a Grant-in-Aid for Scientific Research (B) (No. 24350109) from the Japan Society for the Promotion of Science (JSPS).

Notes and references

[a] Department of Applied Chemistry, Graduate School of Urban Environmental Sciences, Tokyo Metropolitan University, 1-1 Minami-Osawa, Hachioji 192-0397, Japan
*Corresponding author: E-mail: kkaji@tmu.ac.jp

1 T. Komatsu, T. Honma, *Int. J. Appl. Glass Sci.* 2013, **4**, 125.
2 C. Canevali, M. Mattoni, F. Morazzoni, R. Scotti, M. Casu, A. Musinu, R. Krsmanovic, S. Polizzi, A. Speghini, M. Bettinelli, *J. Am. Chem. Soc.* 2005, **127**, 14681.
3 A. Vedda, N. Chiodini, D. D. Martino, M. Fasoli, F. Morazzoni, F. Moretti, R. Scotti, G. Spinolo, A. Baraldi, R. Capelletti, M. Mazzera, M. Nikl, *Chem. Mater.* 2006, **18**, 6178.
4 M. Fasoli, A. Vedda, A. Lauria, F. Moretti, E. Rizzelli, N. Chiodini, F. Meinardi, M. Nikl, *J. Non-Cryst. Solids* 2009, **355**, 1140.
5 S. Mukherjee, C. H. Chen, C. C. Chou, K. F. Tseng, B. K. Chaudhuri, H. D. Yang, *Phys. Rev. B* 2010, **82**, 104107.
6 J. S. Iwanczyk, B. E. Patt, C. R. Tull, L. R. MacDonald, E. Bescher, S. R. Robson, J. D. Mackenzie, E. J. Hoffman, *IEEE Trans. Nucl. Sci.* 2000, **47**, 1781.
7 J. D. Mackenzie, E. P. Bescher, *Acc. Chem. Res.* 2007, **40**, 810.
8 A. Biswas, G. S. Maciel, C. S. Friend, P. N. Prasad, *J. Non-Cryst. Solids* 2003, **316**, 393.
9 V. D. Rodríguez, J. D. Castillo, A. C. Yanes, J. Méndez-Ramos, M. Torres, J. Peraza, *Opt. Mater.* 2007, **29**, 1557.
10 A. C. Yanes, J. J. Velázquez, J. del Castillo, J. Méndez-Ramos, V. D. Rodríguez, *J. Sol-Gel Sci. Technol.* 2009, **51**, 4.

11 A. Santana-Alonso, A. C. Yanes, J. Méndez-Ramos, J. del Castillo, V. D. Rodríguez, *Opt. Mater.* 2011, **33**, 587.
12 S. Nagayama, K. Kajihara, K. Kanamura, *Mater. Sci. Eng. B* 2012, **177**, 510.
13 K. Kajihara, S. Kuwatani, K. Kanamura, *Appl. Phys. Express* 2012, **5**, 012601.
14 K. Kaneko, K. Kajihara, K. Kanamura, *J. Ceram. Soc. Jpn.* 2013, **121**, 299.
15 K. Kajihara, *J. Asian Ceram. Soc.* 2013, **1**, 121.
16 A. Saitoh, S. Murata, S. Matsuishi, M. Oto, T. Miura, M. Hirano, H. Hosono, *Chem. Lett.* 2005, **34**, 1116.
17 A. Saitoh, S. Matsuishi, C. Se-Weon, J. Nishii, M. Oto, M. Hirano, H. Hosono, *J. Phys. Chem. B* 2006, **110**, 7617.
18 B. J. Ainslie, S. P. Craig, S. T. Davey, D. J. Barber, J. R. Taylor, A. S. L. Gomes, *J. Mater. Sci. Lett.* 1987, **6**, 1361.
19 K. Riwotzki, H. Meyssamy, H. Schnablegger, A. Kornowski, M. Haase, *Angew. Chem. Int. Ed.* 2001, **40**, 573
20 K. Kömpe, H. Borchert, J. Storz, A. Lobo, S. Adam, T. Möller, M. Haase, *Angew. Chem. Int. Ed.* 2003, **42**, 5513
21 X. Yu, F. Song, W. Wang, L. Luo, L. Han, Z. Cheng, T. Sun, J. Tian, E. Y. B. Pun, *J. Appl. Phys.* 2008, **104**, 113105
22 H. Guo, F. Li, J. Li, H. Zhang, *J. Am. Ceram. Soc.* 2011, **94**, 1651.
23 Y. Ni, J. M. Hughes, A. N. Mariano, *Am. Mineral.* 1995, **80**, 21.
24 G. M. Begun, G. W. Beall, L. A. Boatner, W. J. Gregor, *J. Raman Spectrosc.* 1981, **11**, 273.
25 E. Nakazawa, *J. Lumin.* 2002, **100**, 89.
26 E. Nakazawa, F. Shiga, *Jpn. J. Appl. Phys.* 2003, **42**, 1642.
27 I. H. Malitson, *J. Opt. Soc. Am.* 1965, **55**, 1205.
28 M. J. Weber, *Handbook of Optical Materials*, *Laser and Optical Science and Technology Series*, CRC Press, Boca Raton, USA, 2003.
29 J. Bourcet, F. K. Fong, *J. Chem. Phys.* 1974, **60**, 34.
30 W. van Schaik, S. Lizzo, W. Smit, G. Blasse, *J. Electrochem. Soc.* 1993, **140**, 216.
31 M. Hirano, S. Shionoya, *J. Phys. Soc. Jpn.* 1972, **33**, 112.
32 U. Kolitsch, D. Holtstam, *Eur. J. Mineral.* 2004, **16**, 117.
33 D. J. Robbins, B. Cockayne, B. Lent, J. L. Glasper, *Solid State Commun.* 1976, **20**, 673.